

Smaller and Faster 3DGS via Post-Training Dictionary Learning

Jiarong Gong, Jonas Unger, Ehsan Miandji
 Linköping University
 Department of Science and technology

jiarong.gong@liu.se, jonas.unger@liu.se, ehsan.miandji@liu.se

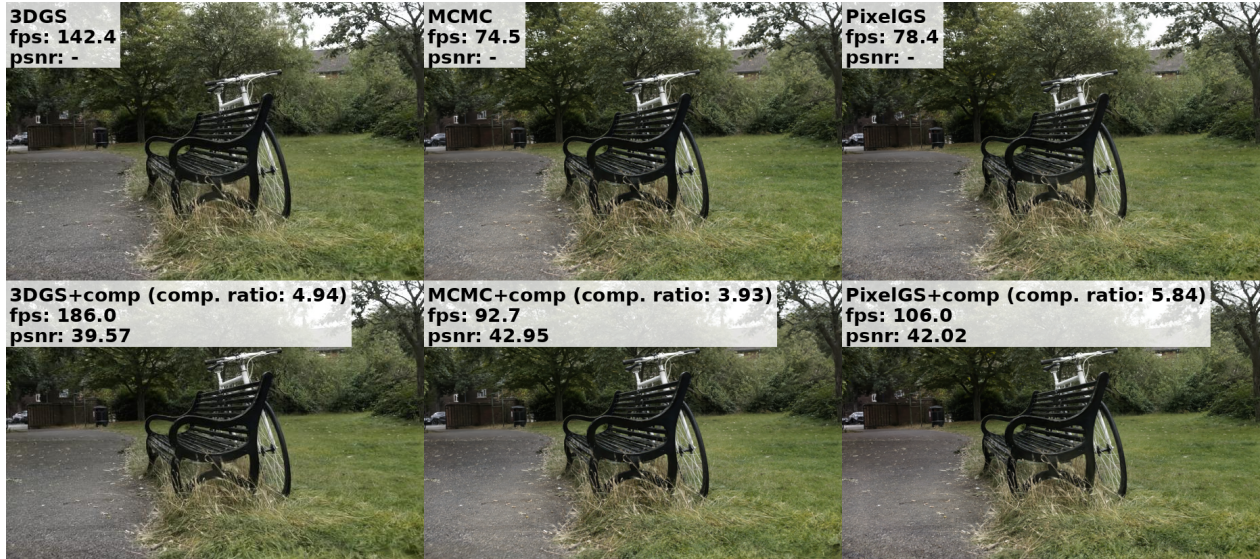


Figure 1. Visual comparison of baseline methods (*3DGS*, *MCMC*, and *PixelGS*, top row) and their compressed counterparts (bottom row). Each panel in bottom row reports the corresponding compression ratio, rendering speed (FPS), and PSNR, highlighting that our dictionary-learning-based compression substantially reduces model size and improves rendering efficiency while preserving visual fidelity. Note that the reported PSNR values here are computed with respect to the renderings of original methods, not the Ground Truth.

Abstract

3D Gaussian Splatting (3DGS) is a promising neural scene representation for real-time rendering, but trained models often suffer from large memory footprints, limiting deployment on less powerful devices. Existing compression techniques often lead to architectures with several additional trainable parameters. While achieving outstanding compression ratios, they introduce noticeable drops in image quality. In this work, we introduce the first dictionary-learning-based compression framework for 3DGS. The proposed post-training compression pipeline can be deployed in virtually any 3DGS model without the need for re-training or modifications to existing 3DGS models. Our compression framework is straightforward to implement, yet provides significant compression capabilities, preserves image quality, and improves real-time render-

ing performance. Across 13 benchmark scenes, our approach achieves an average compression ratio of 3.95 \times , 3.10 \times , and 4.55 \times when applied to 3DGS, 3DGS-MCMC, and PixelGS, respectively. This yields consistent rendering speedups of 23.3%, 24.3%, and 25.3%, while maintaining image quality.

1. Introduction

3D Gaussian Splatting (3DGS) [5] is a radiance field model that enables real-time rendering speed with comparable quality compared to state-of-the-art (SOTA) NeRF methods [2], that has led to a large body of research [6, 12]. 3DGS represents radiance fields using anisotropic Gaussians. While achieving a significant reduction in storage costs when compared to raw radiance field data, the excessive memory costs often hinders its adoption for complex

scenes. As such, 3DGS compression has become an active research field [4, 7, 9, 10]. For instance, Navaneet et al.[10] quantize Gaussian parameters with K-means codebooks and reduce the number of Gaussians of a 3D model via opacity penalization and pruning; Similarly, Girish et al.[4] propose to quantize latent embeddings and prune low-influence Gaussians. However, existing pipelines give rise to a drop in image quality. Additionally, some works concentrate on the reduction of the number of primitives. Fridovich et al.[3] explicitly uses voxel grid to store opacity and spherical harmonics which are used to compute color and makes the voxel grid sparse via voxel pruning. [4, 10] reduces the number of Gaussians by eliminating those with low contributions through opacity, importance score thresholds, etc. For a detailed survey of related work, we refer readers to [1].

In this paper, we propose a fundamentally different approach via a dictionary-learning-based compression pipeline that applies compression as a post-training process, hence enabling compression of existing SOTA 3DGS models with virtually no noticeable degradation in image quality. Since each 3D Gaussian is described by a set of attributes, namely position, covariance, Spherical Harmonics (SH) coefficients for color, and opacity. SH coefficients account for over 80% of the storage cost, we, thus, train a dictionary based on SH coefficients, followed by Orthogonal Matching Pursuit (OMP) [11] to obtain sparse codes. We show that the radiance field reconstruction, e.g. during rendering, can be directly evaluated using the sparse coefficients to obtain directional radiance values. Given the inherent sparsity introduced by our dictionary, our method achieves a higher rendering speed, while reducing the memory footprint and preserving the image quality of a given 3DGS model.

The proposed compression pipeline not only ensures controllable rendering quality via representation sparsity, but also provides flexibility for integration into virtually any 3DGS method. We evaluate this plug-and-play strategy on three SOTA 3DGS methods, and the results consistently demonstrate the effectiveness of our method. To summarize, this paper introduces a 3DGS compression framework with the following contributions:

- We introduce a dictionary learning technology for 3DGS compression that can be applied to existing methods as a light-weight post training process. Our concise representation drastically reduces the storage cost and, equally importantly, maintains image quality.
- With a dictionary and a set of sparse coefficients replacing the SH coefficients, our new sparse rendering algorithm improves the rendering speed by more than 23.3%.

2. Method

2.1. Dictionary Learning and Sparse Representation

We briefly recall the dictionary learning framework, which underpins our compression method. Given a data matrix $X = [x_1, \dots, x_N] \in \mathbb{R}^{d \times N}$, the goal is to find an overcomplete dictionary $D = [a_1, \dots, a_m] \in \mathbb{R}^{d \times m}$, where $m > d$, and sparse codes $\alpha_i \in \mathbb{R}^m, i \in \{1, \dots, N\}$, such that

$$\min_{D, \{\alpha_i\}} \sum_{i=1}^N \|x_i - D\alpha_i\|_2^2, \quad \text{s.t. } \|\alpha_i\|_0 \leq k, \|a_j\|_2 = 1, \forall j. \quad (1)$$

The dictionary learning problem is typically solved approximately via an alternating minimization strategy, whereby the sparse codes $\{\alpha_i\}$ and the dictionary D are updated in turn while keeping the other fixed. Having the dictionary D , and given a new test set, the task is then to obtain the most sparse coefficients while minimizing the error. In our framework, sparse coefficients are achieved via OMP, which efficiently selects the most relevant atoms from the dictionary until either/both a target sparsity k or/and error threshold (tolerance) ϵ is reached. Since $k \ll m$, it has led to several applications in compression, see e.g. [8]. We utilize a learned dictionary, and corresponding sparse coefficients, to compress a subset of 3DGS attributes that exhibit the highest storage/memory cost, as described in what follows.

2.2. Post-training 3DGS compression

Each Gaussian splat in 3DGS is parameterized by its position, covariance, opacity, and SH coefficients. Formally, each Gaussian is described by 59 parameters: 3 for position, 3 for scale, 4 for rotation, 1 for opacity, and 48 for the SH coefficients. This makes SH coefficients the dominant factor in storage overhead.

Our compression strategy targets this issue. Instead of storing all SH coefficients explicitly, we apply learned dictionary and sparse codes to represent SH coefficients in a compact form (with the DC term of SH excluded) after training. Each Gaussian’s SH coefficients are replaced by a shared dictionary and its corresponding sparse codes. For storage, we only need the non-zero elements and their indices for sparse codes. Since each sparse code might have a different number of non-zero elements, we store them in a *Compressed-Sparse-Column* (CSC) format.

To accelerate rendering, we modify the radiance calculation based on the shared dictionary and the corresponding non-zero elements in the sparse codes. In the original computation, it needs to read the whole SH coefficients from global memory while our method reads the small shared dictionary (size: 45×90 FP32, 15.8 KB) and non-zeros of the sparse codes. From our tests (on RTX 4090 and

RTX 4070ti), GPUs are memory-bound devices in terms of radiance computation which means memory-reading takes much more time than radiance computation. Since our method takes smaller information, it costs smaller time than the original. The motivation for acceleration is as follow.

Taking an RTX 4090 as an example, the peak FP32 compute throughput and memory bandwidth are 82.6 TFLOPS and 1008 GB/s, respectively. Under a simplified counting model, the original radiance computation costs about 96 FLOPs per Gaussian, while the compressed version costs about 1,152 FLOPs per Gaussian (about 1,149 FLOPs when the average sparsity is $k = 11.7$). In terms of data movement, the original SH path reads about 192 B per Gaussian, while the compressed path reads about 110 B per Gaussian ($k = 11.7$). The dictionary is a shared 15.8 KB table, accounted for as an amortized term $15.8 \text{ KB}/N_{\text{vis}}$ per frame; due to high cache reuse, this term is negligible for large N_{vis} .

$$\begin{aligned} T_{\text{orig}} &= T_{\text{comp}} + T_{\text{mem}} \\ &= \frac{96}{82.6 \times 10^{12}} + \frac{192}{1008 \times 10^9} \\ &\approx 0.0012 \text{ ns} + 0.1905 \text{ ns} = 0.1917 \text{ ns} \end{aligned} \quad (2)$$

$$\begin{aligned} T_{\text{opt}} &= T_{\text{comp}} + T_{\text{mem}} \\ &= \frac{1152}{82.6 \times 10^{12}} + \frac{110}{1008 \times 10^9} \\ &\approx 0.0139 \text{ ns} + 0.1091 \text{ ns} = 0.1230 \text{ ns} \end{aligned} \quad (3)$$

3. Experiments

3.1. Experimental Setup

Our compressive framework can be easily integrated into SOTA 3DGS methods. To verify the effectiveness of our methods, we make 3 sets of comparisons, *3DGS* [5] vs. *3DGS+comp*, *MCMC*[6] vs. *MCMC+comp*, and *PixelGS*[12] vs. *PixelGS+comp*. All experiments are conducted on an NVIDIA GPU RTX 4090. We report standard evaluation metrics: PSNR, SSIM, and LPIPS for reconstruction quality, compression ratio for storage efficiency, and FPS for rendering speed performance. The experimental scenes include Mip-NeRF-360, Tanks&Temples, and Deep-Blending datasets, 13 scenes in total.

3.2. Effect of Controllable OMP Tolerance Parameter on Rendering Quality and Efficiency

As previously mentioned, the sparsity is controlled by a tolerance parameter when performing OMP algorithm. It, thus, directly decides the quality of the reconstructed SH coefficients and serves as a key factor determining the trade-off between compression ratio and rendering quality. We now investigate how varying the tolerance parameter influences the compressive methods. We study the impact of

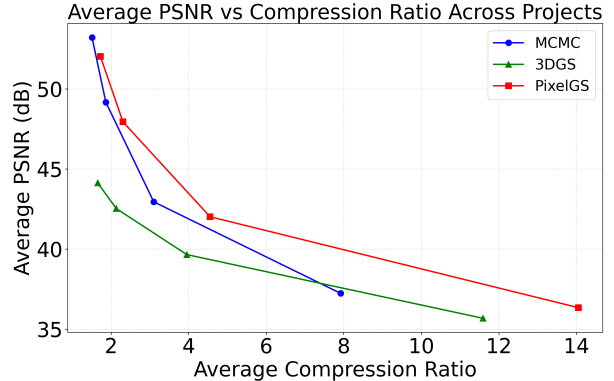


Figure 2. Averaged PSNR vs. Compression Ratio for three SOTA algorithms utilizing our novel post-training compression method.

tolerance by varying it across 0.03, 0.05, 0.1, 0.2, which we selected based on preliminary experiments showing that these values cover the typical trade-off range between high-fidelity reconstruction and aggressive compression. For better understanding, we use compression ratio as an indicator of tolerance in the following figures.

Figure 2 (more figures per scene for the 3 SOTA 3DGS methods can be found in **Supplementary Material** Section 1) plots PSNR against compression ratio, revealing the expected degradation in quality as compression increases. However the rate of degradation diminishes. Extrapolating this trend, we anticipate that quality will ultimately plateau: once compression is sufficiently strong, the sparse codes finally have a single non-zero entry whose value remains fixed; consequently, the SH-coefficient reconstruction error reaches its upper bound and ceases to grow. Note that the reported PSNR values are computed with respect to original renderings, not the GT. Thus, it basically indicates the visual similarity between baselines and their compressive counterparts.

Tolerance also affects the rendering speed. Figure 3 (see more figures in **Supplementary Material** Section 2) quantify the trade-off between compression strength and rendering speed, plotting FPS against compression ratio. Figure 3 shows the frame-rate rises monotonically with stronger compression, but the rendering efficiency gain diminishes and the curves eventually plateau. This saturation aligns with the quality analysis given previously.

To further quantify the rendering fidelity and efficiency of our compression method, Table 2 reports PSNR, SSIM, Lpips, and FPS means over each scene for the compressed renderings of each pipeline *3DGS+comp*, *MCMC+comp*, and *PixelGS+comp* at tolerance 0.1, against the corresponding original baseline renderings. A table records the same metric results over different tolerances is included in **Supplementary Material** Section 3. From Table 2, it is evident that our method preserves rendering quality since the min-

Table 1. Mean per-scene PSNR (dB), SSIM, LPIPS, and FPS of compressive renderings relative to the original for tol = 0.10. Higher PSNR/SSIM and lower LPIPS indicate closer agreement with the original. "FPS(-Comp)" denotes the rendering speed of the original baselines.

Method	Metric	Bicycle	Bonsai	Counter	Garden	Kitchen	Room	Stump	Truck	Flowers	Playroom	Train	Treehill	Drjohnson	Mean
3DGS+comp	PSNR	38.54	41.03	40.69	37.97	39.59	41.20	38.51	39.34	37.80	40.03	39.64	39.18	40.84	39.57
	SSIM	0.9830	0.9863	0.9818	0.9810	0.9851	0.9829	0.9819	0.9859	0.9870	0.9821	0.9873	0.9829	0.9871	0.9842
	LPIPS	0.0301	0.0264	0.0263	0.0296	0.0217	0.0301	0.0392	0.0210	0.0257	0.0260	0.0210	0.0311	0.0311	0.0276
	Comp Ratio	4.94	4.65	3.76	3.16	3.36	4.91	4.15	3.92	3.40	3.56	3.39	3.76	4.33	3.95
	FPS	186.0	268.9	186.7	223.7	158.8	186.9	197.1	225.9	305.7	203.2	193.2	203.7	173.4	208.7
	FPS(-Comp)	142.4	240.0	170.5	188.4	143.9	167.7	147.7	193.4	250.4	177.7	178.6	163.6	136.2	169.3
MCMC+comp	PSNR	43.20	43.09	43.56	42.85	42.64	43.64	44.21	42.51	43.41	42.17	42.29	43.22	41.57	42.95
	SSIM	0.9974	0.9951	0.9947	0.9969	0.9964	0.9944	0.9966	0.9969	0.9974	0.9946	0.9970	0.9967	0.9952	0.9961
	LPIPS	0.0094	0.0067	0.0065	0.0080	0.0060	0.0056	0.0126	0.0051	0.0076	0.0045	0.0062	0.0096	0.0109	0.0076
	Comp Ratio	3.93	3.22	2.67	2.85	2.64	3.72	2.80	3.29	2.25	2.54	3.43	3.38	3.56	3.10
	FPS	92.7	182.3	125.5	101.5	129.7	142.5	92.1	148.8	74.1	182.3	216.5	85.3	253.2	140.5
	FPS(-Comp)	74.5	167.1	118.5	82.9	118.0	132.2	78.4	127.7	67.6	157.1	196.5	72.4	177.6	113.0
PixelGS+comp	PSNR	42.41	42.18	42.73	41.97	41.85	42.11	42.78	41.65	42.24	41.20	41.50	42.00	41.61	42.02
	SSIM	0.9954	0.9932	0.9914	0.9950	0.9948	0.9913	0.9943	0.9952	0.9958	0.9915	0.9958	0.9945	0.9940	0.9940
	LPIPS	0.0123	0.0115	0.0101	0.0104	0.0086	0.0152	0.0164	0.0078	0.0106	0.0114	0.0084	0.0140	0.0164	0.0118
	Comp Ratio	5.84	5.13	4.40	3.56	3.69	5.53	4.36	4.56	3.59	4.45	4.29	4.18	5.59	4.55
	FPS	106.0	216.0	123.9	138.0	129.4	158.5	116.8	117.7	114.4	152.5	119.9	97.3	134.5	132.7
	FPS(-Comp)	78.4	183.5	106.9	105.6	107.5	133.0	88.1	93.1	89.6	122.9	99.0	73.8	95.3	105.9

imum PSNR value is 37.80 dB and the maximum PSNR 44.21 dB; from **Metric** "Comp Ratio" and "FPS", we can also easily find that across all frameworks, our method consistently reduces memory usage and improves rendering efficiency. More concretely, when our compressive framework is applied to baselines, our method improves the rendering speed substantially, with average FPS gains of 23.3%, 24.3%, and 25.3%. Meanwhile, the SH coefficients achieve significant compression, with mean ratios of $3.95\times$, $3.10\times$, and $4.55\times$, respectively.

To ensure a rigorous evaluation, we further benchmark our framework against Ground Truth (GT) images across three SOTA methods. As detailed in **Supplementary Material** Section 4, the performance gap between our compressed models and the original baselines is negligible, e.g., with an average PSNR decrease of 0.14 dB for 3DGS. In contrast, existing methods like EAGLES [4] incur more pronounced quality degradation (e.g., a 0.21 dB average PSNR drop) and significant performance volatility in complex scenes (e.g., up to 0.76 dB and 0.62 dB drops in Bonsai and Counter, respectively) due to Scalar Quantization. Notably, unlike our streamlined post-training approach, EAGLES requires a burdensome optimization process via Quantization-Aware Training (QAT). This necessitates the Straight-Through Estimator (STE) to bypass non-differentiable gradients, which significantly increases implementation complexity and computational overhead.

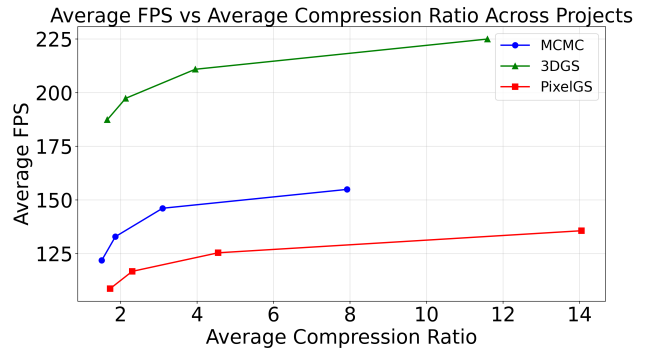


Figure 3. Averaged FPS vs. Compression Ratio for three SOTA algorithms. *PixelGS* presents a stronger compression than the other two.

4. Conclusion

In this paper, we presented the first dictionary-learning-based post-training compression framework for 3D Gaussian Splatting. This approach brings benefits in two dimensions. First, dictionary-learning compression significantly reduces the number of Gaussian parameters, achieving compression ratios of $3.95\times$, $3.10\times$, and $4.55\times$ for 3DGS, 3DGS-MCMC, and PixelGS, respectively, while preserving rendering fidelity. Second, leveraging the compact representation, we optimized the rasterization process, leading to consistent rendering speedups of more than 23% across all frameworks. These improvements confirm that dictionary learning provides an effective and generalizable compression strategy for Gaussian splatting methods.

References

- [1] Milena T Bagdasarian, Paul Knoll, Y Li, Florian Barthel, Anna Hilsmann, Peter Eisert, and Wieland Morgenstern. 3dgs. zip: A survey on 3d gaussian splatting compression methods. In *Computer Graphics Forum*, page e70078. Wiley Online Library, 2025. [2](#)
- [2] Jonathan T Barron, Ben Mildenhall, Dor Verbin, Pratul P Srinivasan, and Peter Hedman. Zip-nerf: Anti-aliased grid-based neural radiance fields. In *Proceedings of the IEEE/CVF International Conference on Computer Vision*. [1](#)
- [3] Sara Fridovich-Keil, Alex Yu, Matthew Tancik, Qinhong Chen, Benjamin Recht, and Angjoo Kanazawa. Plenoxels: Radiance fields without neural networks. In *Proceedings of the IEEE/CVF conference on computer vision and pattern recognition*. [2](#)
- [4] Sharath Girish, Kamal Gupta, and Abhinav Shrivastava. Eagles: Efficient accelerated 3d gaussians with lightweight encodings. In *European Conference on Computer Vision*. [2](#), [4](#)
- [5] Bernhard Kerbl, Georgios Kopanas, Thomas Leimkühler, and George Drettakis. 3d gaussian splatting for real-time radiance field rendering. *ACM Trans. Graph.* [1](#), [3](#)
- [6] Shakiba Kheradmand, Daniel Rebain, Gopal Sharma, Weiwei Sun, Yang-Che Tseng, Hossam Isack, Abhishek Kar, Andrea Tagliasacchi, and Kwang Moo Yi. 3d gaussian splatting as markov chain monte carlo. *Advances in Neural Information Processing Systems*. [1](#), [3](#)
- [7] Joo Chan Lee, Daniel Rho, Xiangyu Sun, Jong Hwan Ko, and Eunbyung Park. Compact 3d gaussian representation for radiance field. In *Proceedings of the IEEE/CVF Conference on Computer Vision and Pattern Recognition*, pages 21719–21728, 2024. [2](#)
- [8] Ehsan Miandji, Saghi Hajisharif, and Jonas Unger. A unified framework for compression and compressed sensing of light fields and light field videos. *38(3)*, 2019. [2](#)
- [9] Wieland Morgenstern, Florian Barthel, Anna Hilsmann, and Peter Eisert. Compact 3d scene representation via self-organizing gaussian grids. In *European Conference on Computer Vision*, pages 18–34. Springer, 2024. [2](#)
- [10] KL Navaneet, Kossar Pourahmadi Meibodi, Soroush Abbasi Koohpayegani, and Hamed Pirsiavash. Compact3d: Smaller and faster gaussian splatting with vector quantization. [2](#)
- [11] Yagyensh Chandra Pati, Ramin Rezaifar, and Perinkulam Sambamurthy Krishnaprasad. Orthogonal matching pursuit: Recursive function approximation with applications to wavelet decomposition. In *Proceedings of 27th Asilomar conference on signals, systems and computers*. [2](#)
- [12] Zheng Zhang, Wenbo Hu, Yixing Lao, Tong He, and Hengshuang Zhao. Pixel-gs: Density control with pixel-aware gradient for 3d gaussian splatting. In *European Conference on Computer Vision*. [1](#), [3](#)

Supplementary Material

Smaller and Faster 3D Gaussian Splatting via Post-Training Dictionary Learning

This supplementary material contains additional qualitative and quantitative per-scene results referenced in the main paper. There are 13 scenes in total, but here we only present results on 8 scenes to make this supplementary file $\leq 10\text{MB}$ which is the upper limit size of a file uploaded through submission system

1. The Effect of Compression Ratio on the Rendered Image Quality

Here we provide additional figures illustrating the effect of compression ratio (controlled by the OMP tolerance) on rendered image quality, measured in PSNR, across 13 scenes. In total, our evaluation covers 13 scenes for each of the three baselines combined with our compression method (*3DGS+comp*, *MCMC+comp*, and *PixelGS+comp*). “Max PSNR” and “Min PSNR” are obtained by evaluating the renderings from all test camera viewpoints. For instance, the **Bicycle** scene contains 25 test cameras, and the reported Max/Min PSNR corresponds to the highest and lowest PSNR among these views.

1.1. 3DGS+Comp

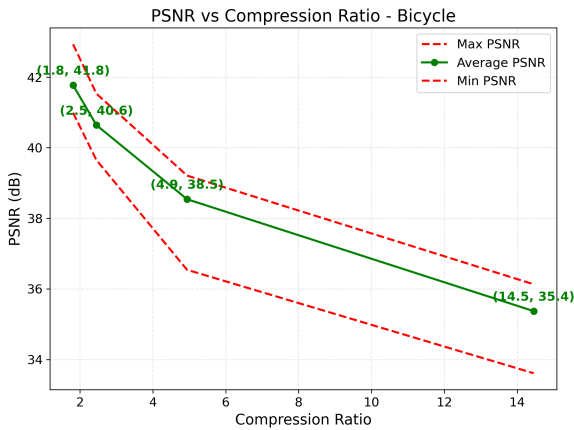


Figure 4. Effect of compression ratio on rendering quality for the *Bicycle* scene.

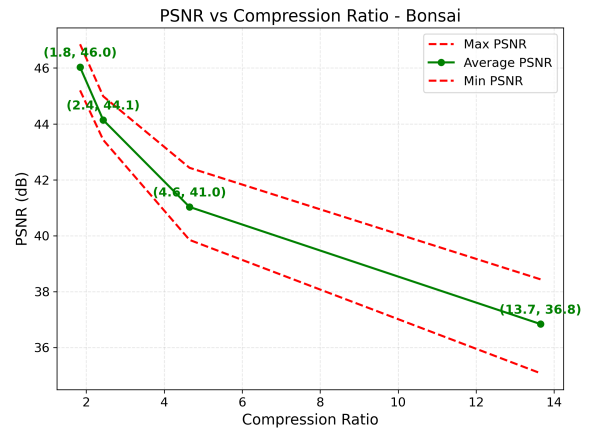


Figure 5. Effect of compression ratio on rendering quality for the *Bonsai* scene.

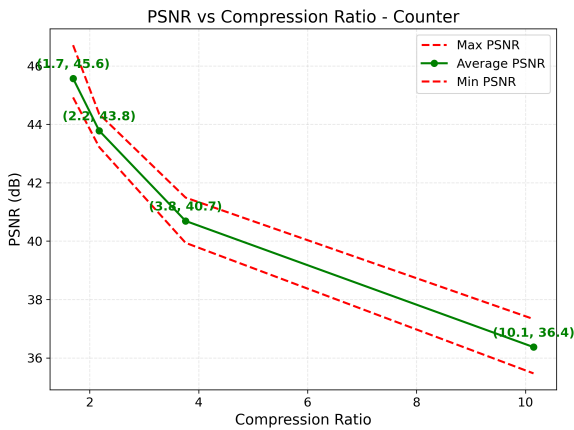


Figure 6. Effect of compression ratio on rendering quality for the *Counter* scene.

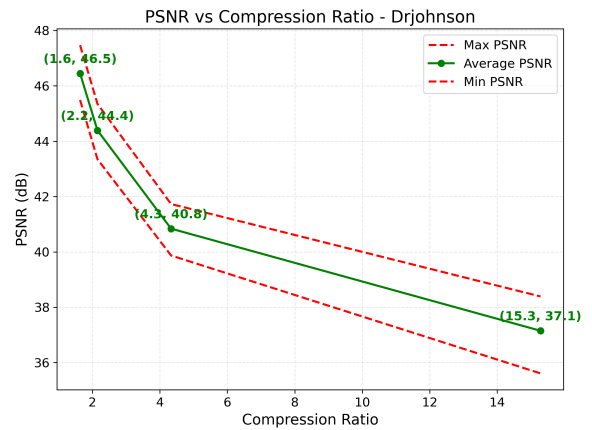


Figure 7. Effect of compression ratio on rendering quality for the *Drjohnson* scene.

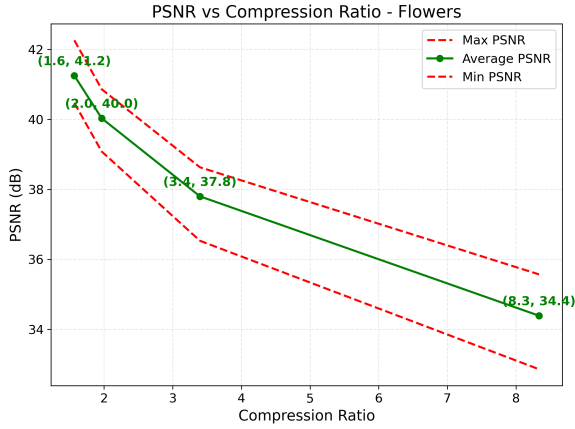


Figure 8. Effect of compression ratio on rendering quality for the *Flowers* scene.

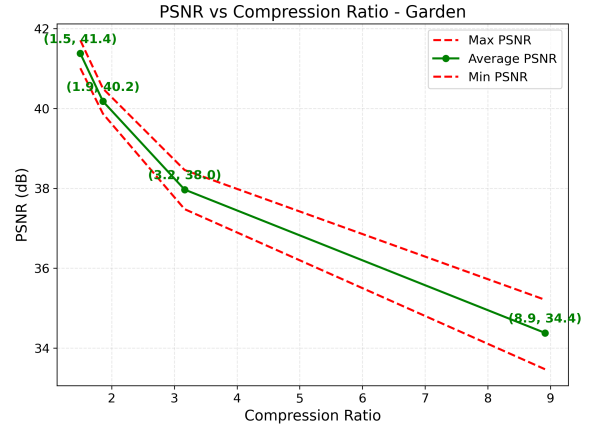


Figure 9. Effect of compression ratio on rendering quality for the *Garden* scene.

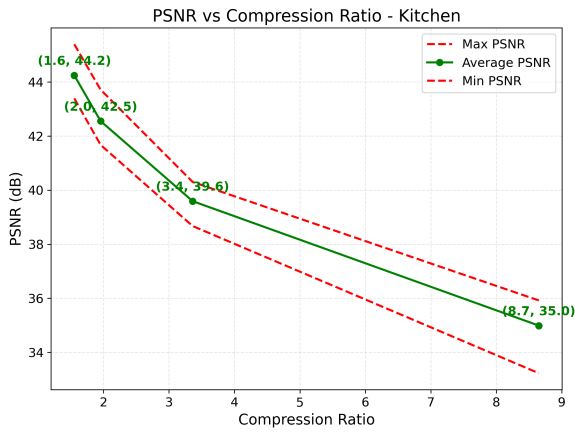


Figure 10. Effect of compression ratio on rendering quality for the *Kitchen* scene.

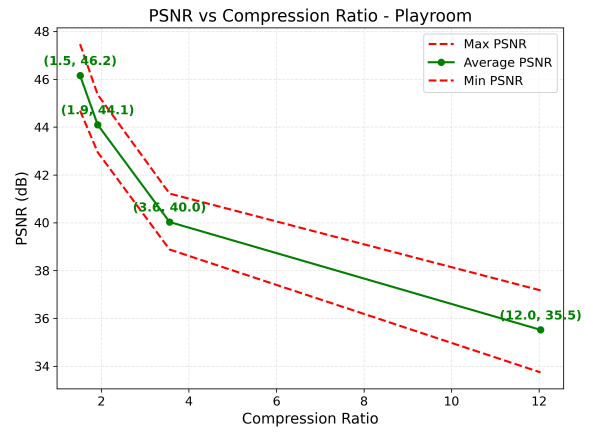


Figure 11. Effect of compression ratio on rendering quality for the *Playroom* scene.

1.2. MCMC+Comp

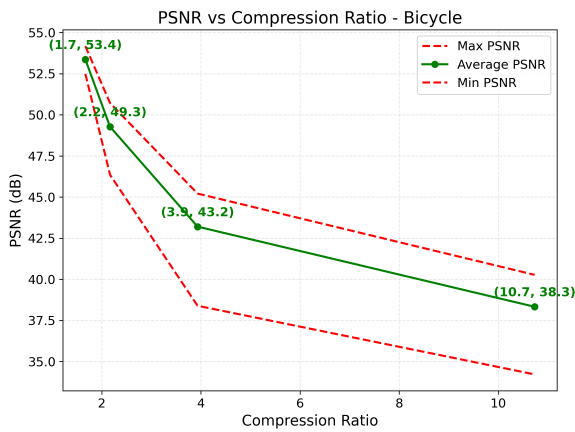


Figure 12. Effect of compression ratio on rendering quality for the *Bicycle* scene.

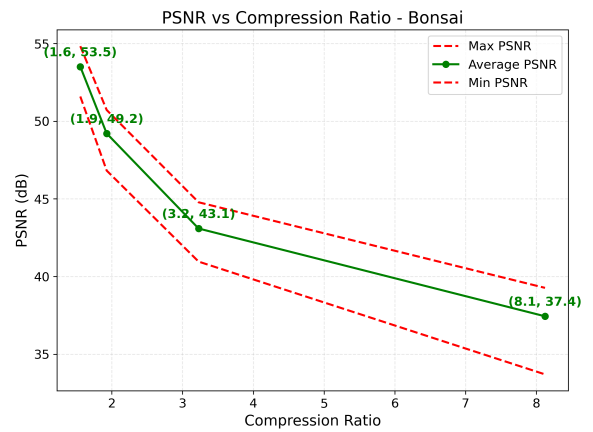


Figure 13. Effect of compression ratio on rendering quality for the *Bonsai* scene.

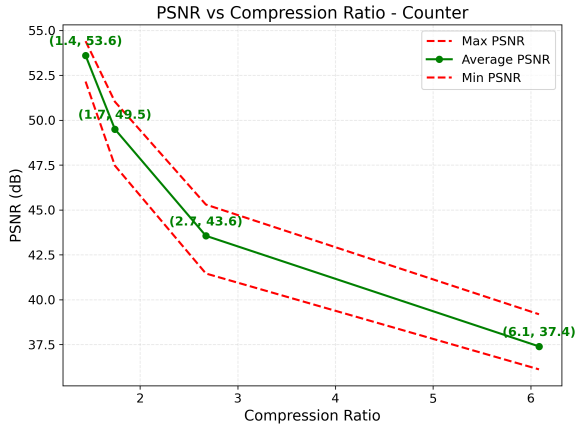


Figure 14. Effect of compression ratio on rendering quality for the *Counter* scene.

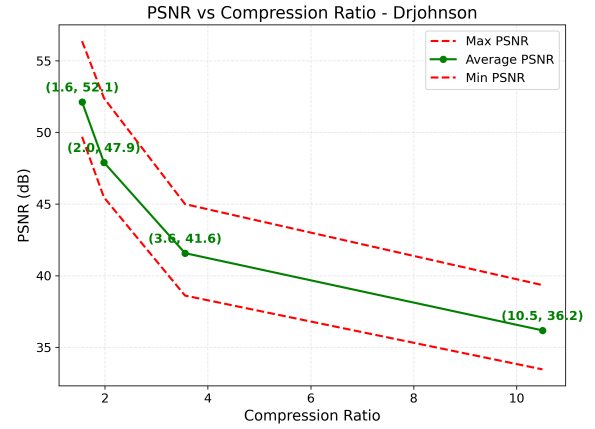


Figure 15. Effect of compression ratio on rendering quality for the *Drjohnson* scene.

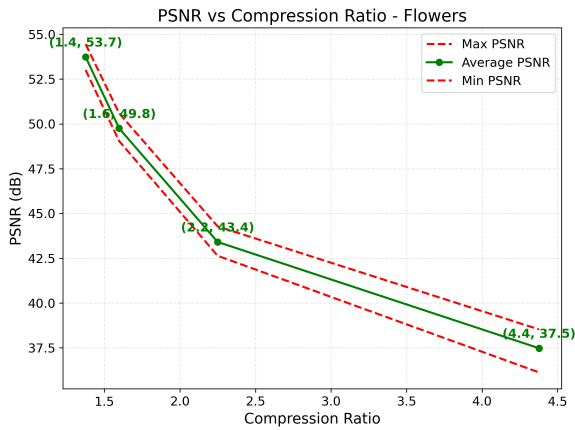


Figure 16. Effect of compression ratio on rendering quality for the *Flowers* scene.

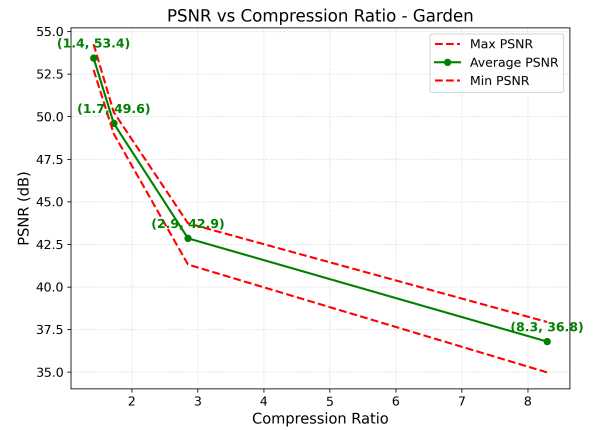


Figure 17. Effect of compression ratio on rendering quality for the *Garden* scene.

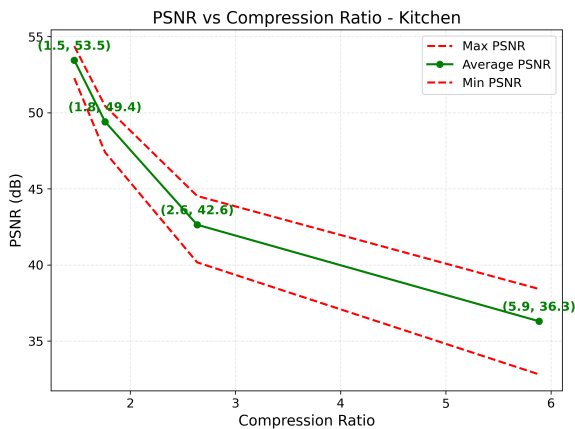


Figure 18. Effect of compression ratio on rendering quality for the *Kitchen* scene.

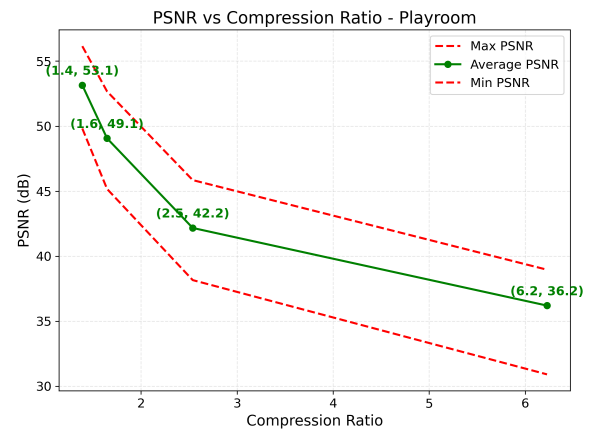


Figure 19. Effect of compression ratio on rendering quality for the *Playroom* scene.

1.3. PixelGS+Comp

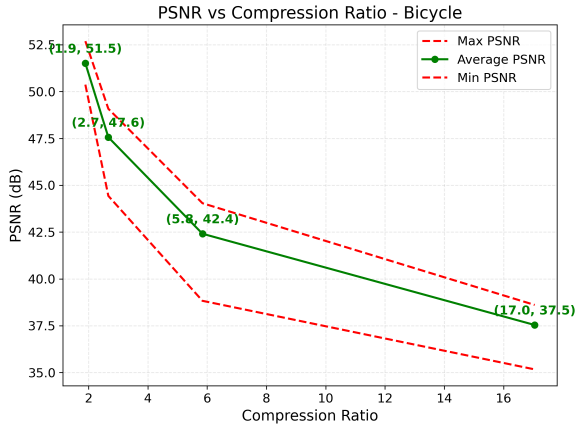


Figure 20. Effect of compression ratio on rendering quality for the *Bicycle* scene.

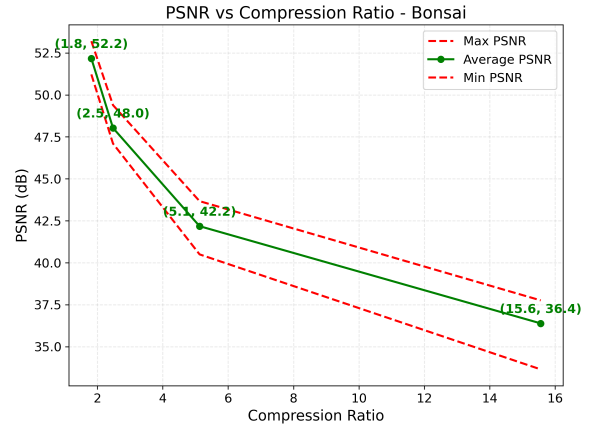


Figure 21. Effect of compression ratio on rendering quality for the *Bonsai* scene.

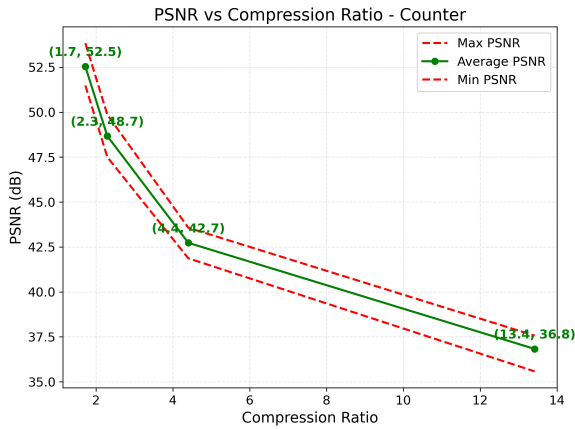


Figure 22. Effect of compression ratio on rendering quality for the *Counter* scene.

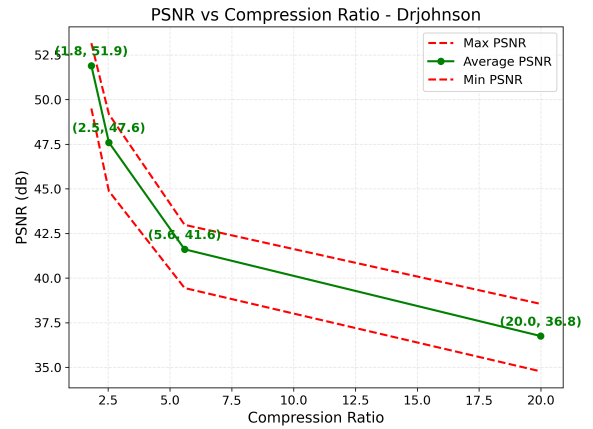


Figure 23. Effect of compression ratio on rendering quality for the *Drjohnson* scene.

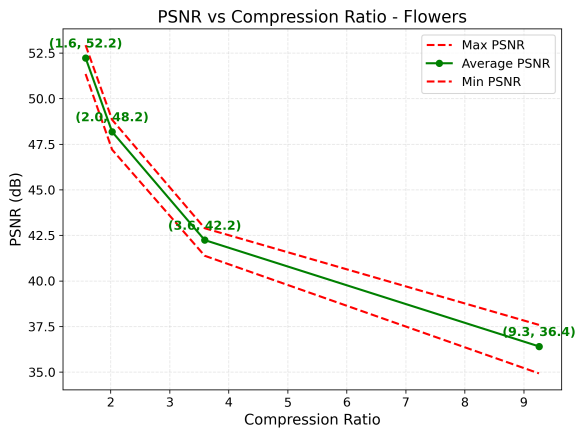


Figure 24. Effect of compression ratio on rendering quality for the *Flowers* scene.

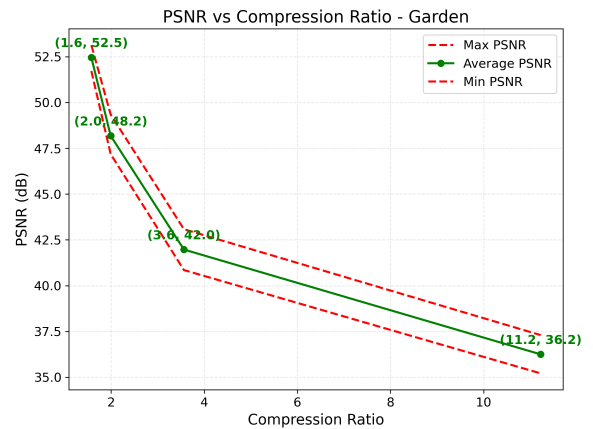


Figure 25. Effect of compression ratio on rendering quality for the *Garden* scene.

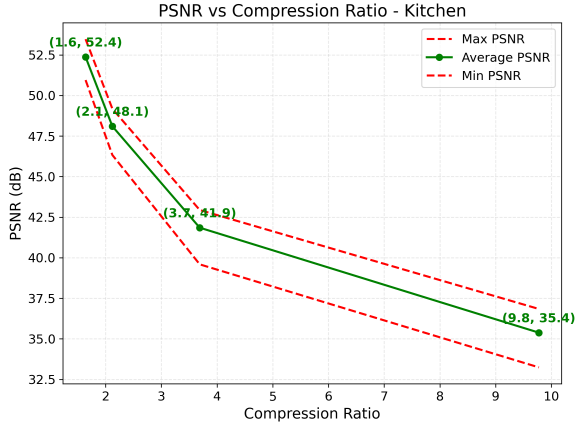


Figure 26. Effect of compression ratio on rendering quality for the *Kitchen* scene.

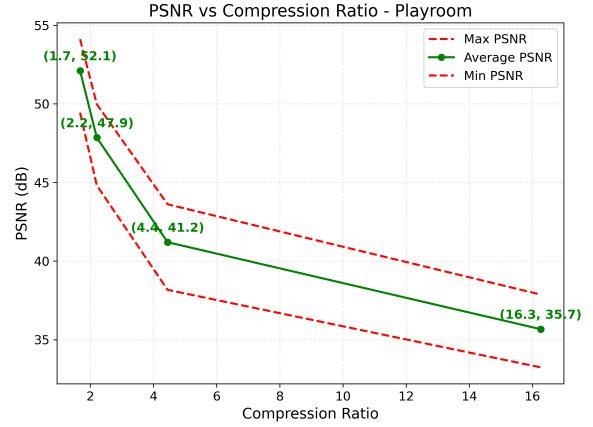
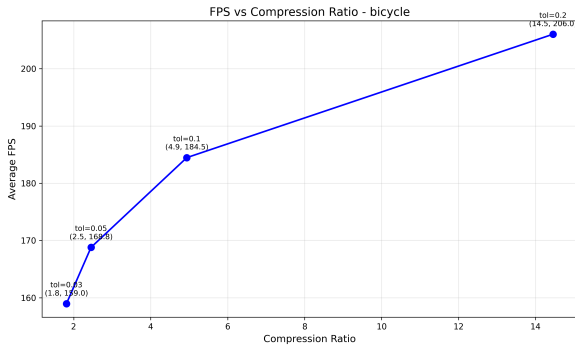


Figure 27. Effect of compression ratio on rendering quality for the *Playroom* scene.

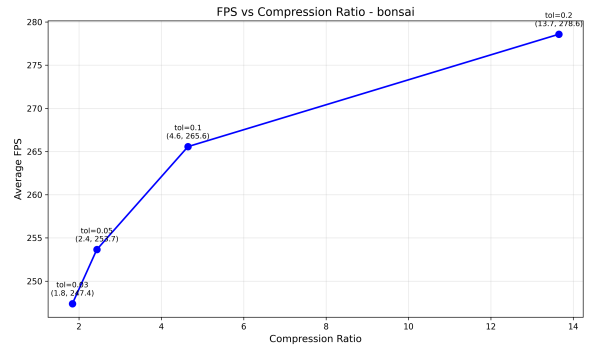
2. Rendering Speed vs. Compression Ratio: Cross-Scene and Cross-Method Evaluation

Here we present, for every test scene and all three methods, the measured rendering throughput (FPS) as a function of compression ratio.

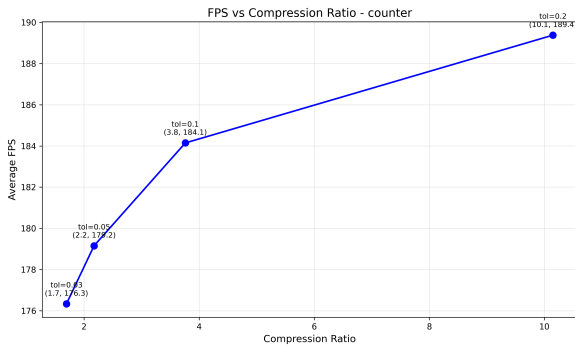
2.1. 3DGS+Comp



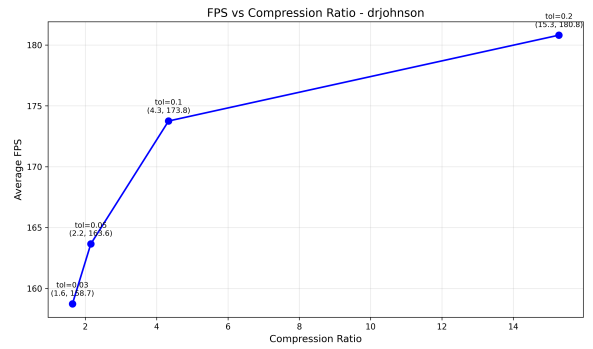
Bicycle



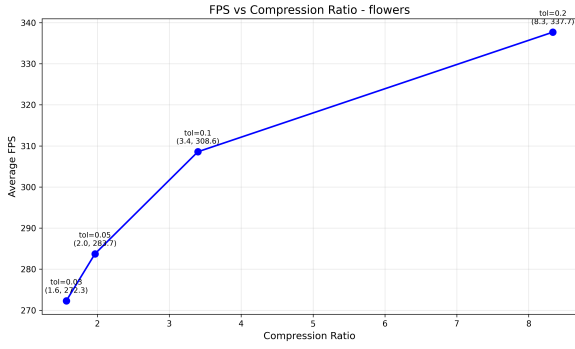
Bonsai



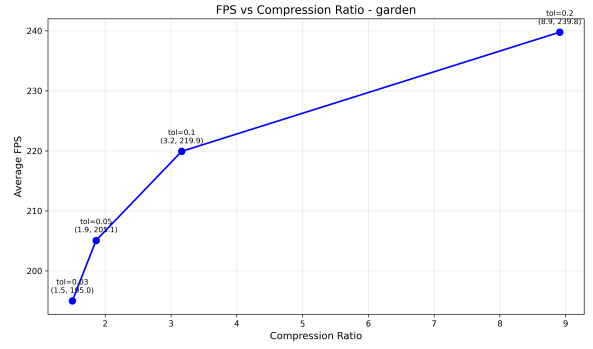
Counter



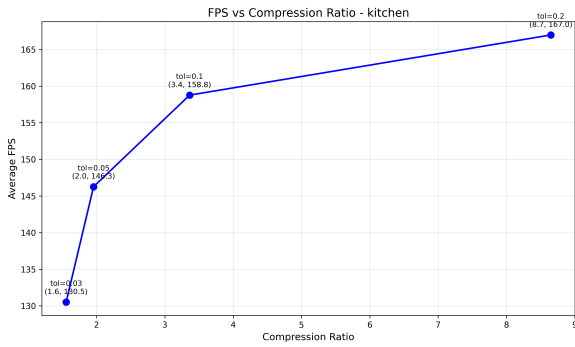
Drjohnson



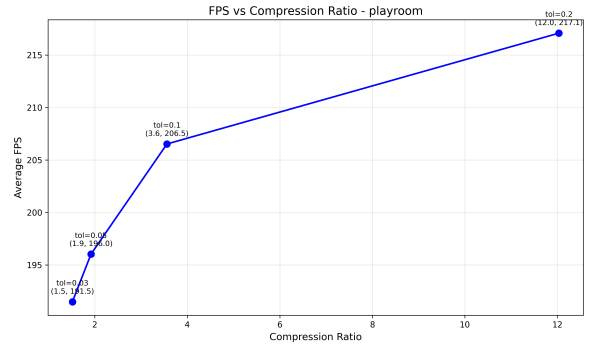
Flowers



Garden

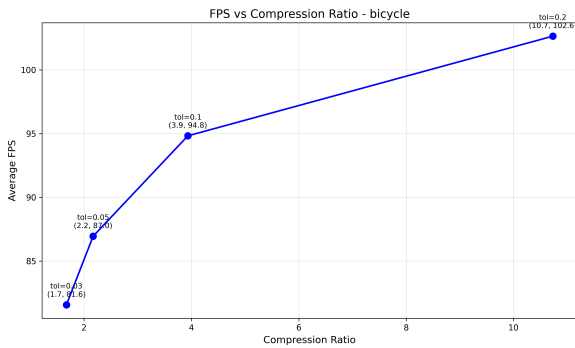


Kitchen

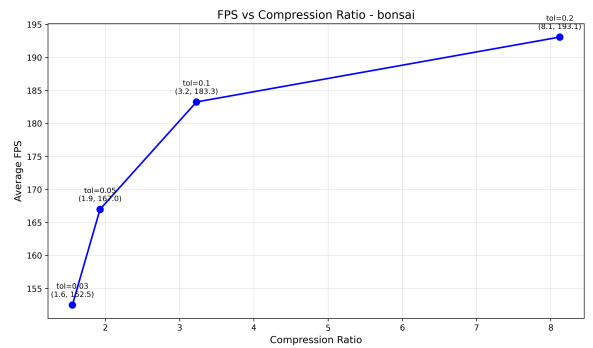


Playroom

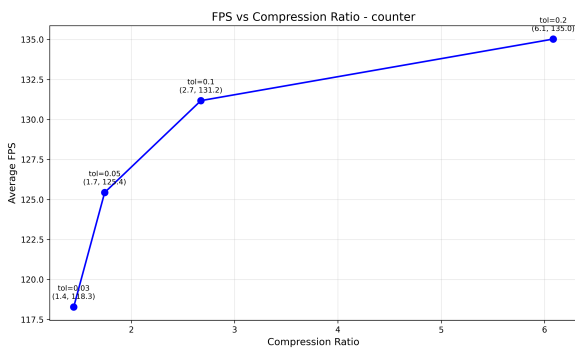
2.2. MCMC+Comp



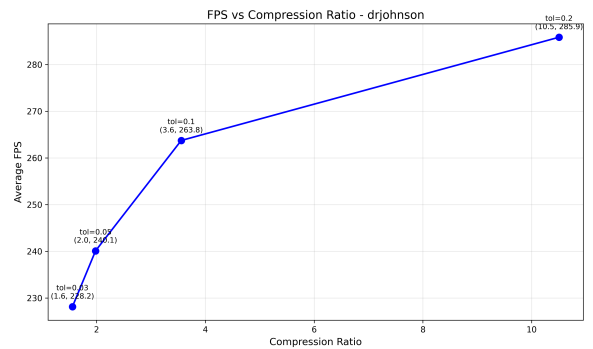
Bicycle



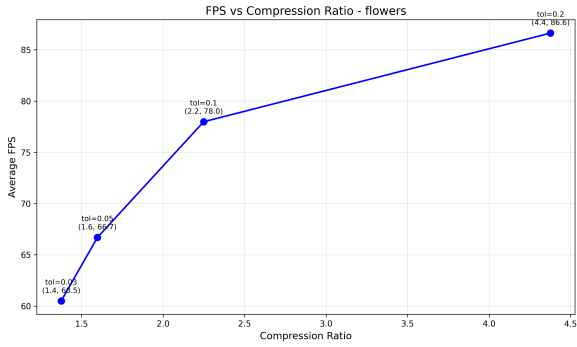
Bonsai



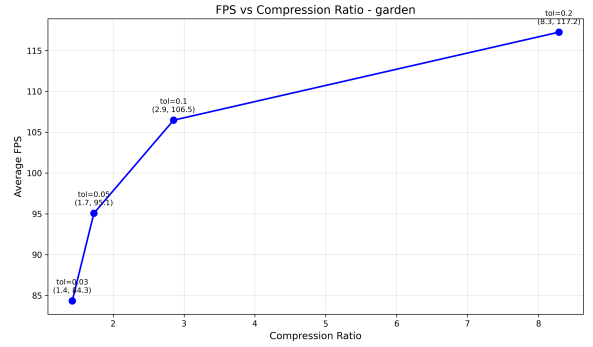
Counter



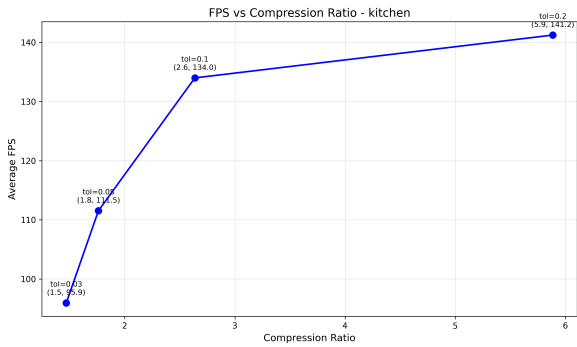
Drjohnson



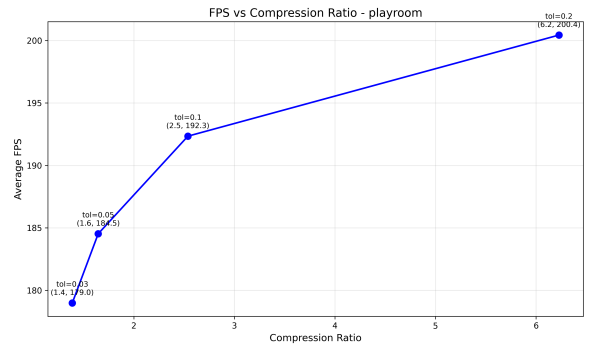
Flowers



Garden

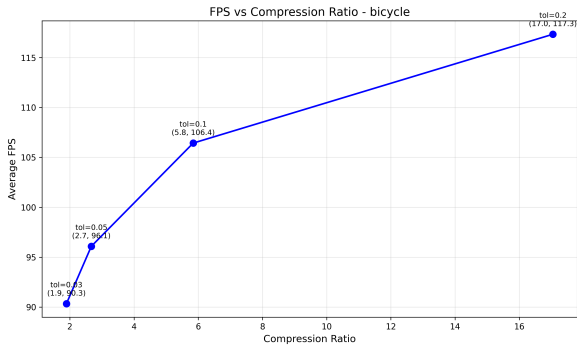


Kitchen

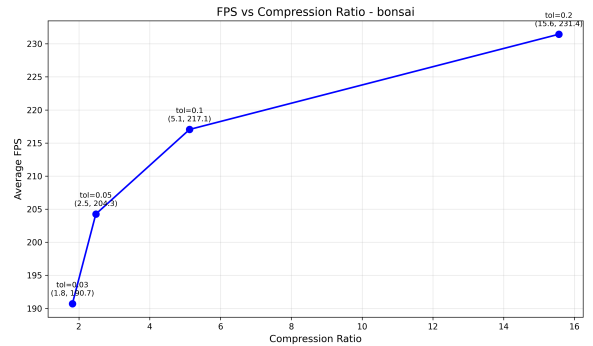


Playroom

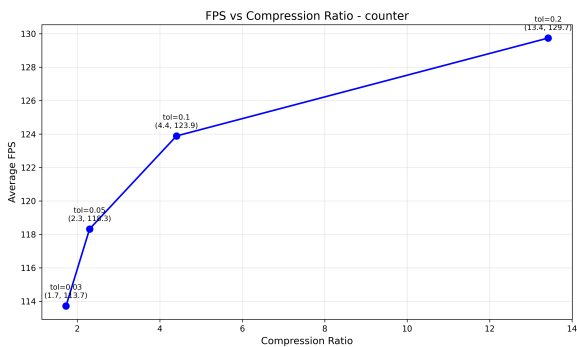
2.3. PixelGS+Comp



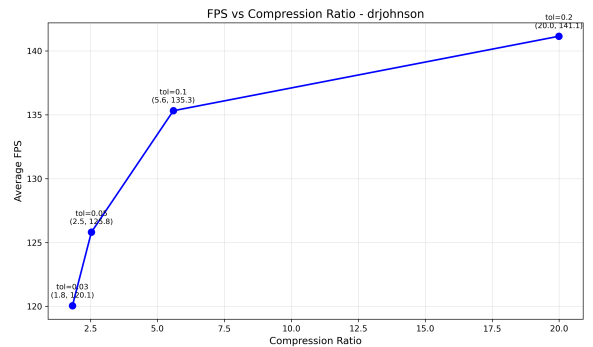
Bicycle



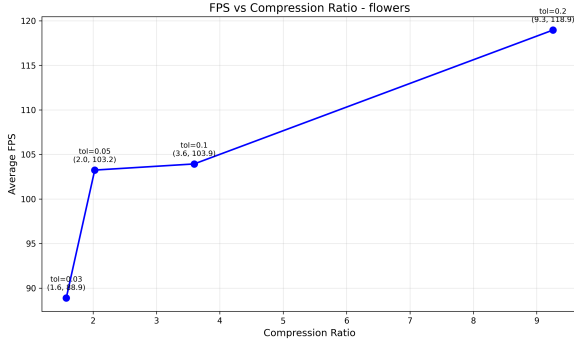
Bonsai



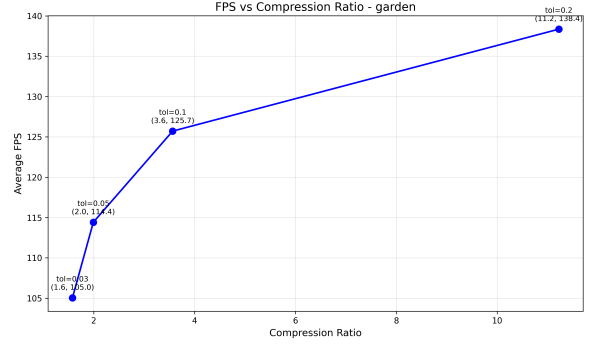
Counter



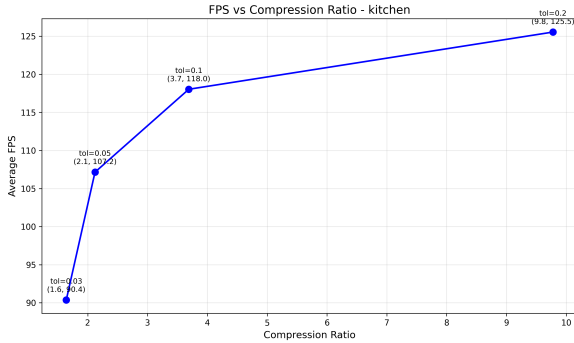
Drjohnson



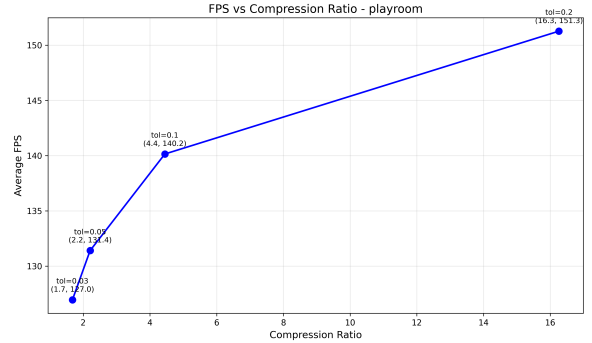
Flowers



Garden



Kitchen



Playroom

3. Quantitative Evaluation of Rendering Fidelity Across Tolerance Levels

To quantify the rendering fidelity of our compression method and have a deeper understanding of the effect of the tolerance, Table 2 reports PSNR, SSIM, and LPIPS means over each scene for the compressed renderings of each pipeline *3DGS+comp*, *MCMC+comp*, and *PixelGS+comp* at different tolerance levels (tol = 0.03, 0.05, 0.1, 0.2), against the corresponding original baseline renderings. From Table 2, we can easily find the same conclusions that as the tolerance value increases (which leads to sparser representations and thus stronger compression), the rendering quality gradually decreases.

4. Quantitative Evaluation of Rendering Quality with respect to GT

To ensure a rigorous and standardized evaluation, we assess the performance of our compression framework by measuring rendering metrics against Ground Truth (GT) images. Table 3 presents a comprehensive per-scene comparison across three SOTA baselines (3DGS, 3DGS-MCMC, and PixelGS) and the competitive EAGLES method.

Experimental results in Table 3 demonstrate that our framework maintains high rendering fidelity across diverse SOTA methods. Notably, our framework is method-agnostic and can be seamlessly integrated as a plug-and-play module. On average, the PSNR degradation remains within a marginal range of 0.14 to 0.19 dB, with negligible impacts on SSIM and LPIPS, illustrating a near-lossless preservation of visual quality post-compression.

Furthermore, our framework exhibits superior stability across various base architectures. While compression often introduces artifacts in complex geometries, our scheme incurs only marginal fidelity loss even in the most challenging scenarios. For instance, when integrated with 3DGS, the maximum per-scene PSNR drop is strictly capped at 0.37 dB; across all evaluated methods, the worst-case degradation remains below 0.52 dB. In stark contrast, EAGLES’ SQ exhibits significant instability. Its PSNR plunges by as much as 0.76 dB in the “Bonsai” scene and exceeds 0.6 dB in “Counter” and “Kitchen.” These results highlight the robustness of our framework in preserving scene-specific details without the unpredictable volatility inherent in existing quantization baselines.

Beyond rendering quality, our framework offers significant advantages in simplicity and efficiency. Unlike EAGLES, which relies on Quantization-Aware Training (QAT) and necessitates the Straight-Through Estimator (STE) to bypass non-differentiability, our method is a strictly post-training compression scheme. Specifically, EAGLES requires modifying gradient propagation, imposing heavy training overhead and implementation complexity. In contrast, our approach can be directly applied to any pre-trained model without further tuning. This nature makes our framework a more scalable solution for

Table 2. Mean per-scene PSNR (dB), SSIM and LPIPS of compressed renderings relative to original renderings at four tolerance levels (tol = 0.03, 0.05, 0.10, 0.20). Higher PSNR/SSIM and lower LPIPS indicate closer agreement with the original.

Method	tol	Metric	Bicycle	Bonsai	Counter	Garden	Kitchen	Room	Stump	Truck	Flowers	Playroom	Train	Treehill	Drjohnson	Mean
3DGS+comp	tol=0.03	PSNR	41.77	46.03	45.57	41.38	44.24	46.33	41.85	43.43	41.25	46.16	44.19	42.69	46.45	43.95
		SSIM	0.9898	0.9930	0.9909	0.9893	0.9921	0.9917	0.9906	0.9918	0.9928	0.9912	0.9930	0.9902	0.9931	0.9915
		LPIPS	0.0176	0.0149	0.0144	0.0156	0.0113	0.0170	0.0190	0.0124	0.0134	0.0148	0.0111	0.0180	0.0171	0.0151
	tol=0.05	PSNR	40.64	44.14	43.78	40.18	42.55	44.53	40.70	41.90	40.03	44.10	42.58	41.45	44.39	42.38
		SSIM	0.9881	0.9906	0.9878	0.9869	0.9898	0.9890	0.9883	0.9897	0.9910	0.9881	0.9909	0.9883	0.9910	0.9892
		LPIPS	0.0214	0.0193	0.0188	0.0198	0.0148	0.0211	0.0252	0.0153	0.0171	0.0185	0.0146	0.0219	0.0219	0.0192
	tol=0.10	PSNR	38.54	41.03	40.69	37.97	39.59	41.20	38.51	39.34	37.80	40.03	39.64	39.18	40.84	39.57
		SSIM	0.9830	0.9863	0.9818	0.9810	0.9851	0.9829	0.9819	0.9859	0.9870	0.9821	0.9873	0.9829	0.9871	0.9842
		LPIPS	0.0301	0.0264	0.0263	0.0296	0.0217	0.0301	0.0392	0.0210	0.0257	0.0260	0.0210	0.0311	0.0311	0.0276
	tol=0.20	PSNR	35.37	36.84	36.37	34.38	34.99	36.96	35.27	35.40	34.39	35.52	35.28	35.54	37.15	35.65
		SSIM	0.9656	0.9772	0.9691	0.9629	0.9730	0.9708	0.9638	0.9768	0.9764	0.9725	0.9793	0.9643	0.9799	0.9717
		LPIPS	0.0510	0.0408	0.0425	0.0506	0.0382	0.0492	0.0647	0.0331	0.0449	0.0421	0.0331	0.0563	0.0472	0.0457
MCMC+comp	tol=0.03	PSNR	53.36	53.51	53.60	53.44	53.45	52.86	53.86	53.01	53.74	53.15	53.28	52.46	52.12	53.22
		SSIM	0.9993	0.9984	0.9984	0.9993	0.9989	0.9982	0.9994	0.9988	0.9995	0.9982	0.9989	0.9991	0.9980	0.9988
		LPIPS	0.0012	0.0012	0.0010	0.0008	0.0008	0.0013	0.0013	0.0008	0.0008	0.0010	0.0008	0.0015	0.0017	0.0011
	tol=0.05	PSNR	49.27	49.21	49.50	49.60	49.41	49.19	50.01	48.82	49.75	49.06	48.97	48.54	47.90	49.17
		SSIM	0.9989	0.9976	0.9975	0.9989	0.9985	0.9975	0.9989	0.9984	0.9991	0.9976	0.9984	0.9986	0.9975	0.9983
		LPIPS	0.0031	0.0027	0.0022	0.0021	0.0019	0.0023	0.0037	0.0017	0.0022	0.0017	0.0019	0.0035	0.0037	0.0025
	tol=0.10	PSNR	43.20	43.09	43.56	42.85	42.64	43.64	44.21	42.51	43.41	42.17	42.29	43.22	41.57	42.95
		SSIM	0.9974	0.9951	0.9947	0.9969	0.9964	0.9944	0.9966	0.9969	0.9974	0.9946	0.9970	0.9967	0.9952	0.9961
		LPIPS	0.0094	0.0067	0.0065	0.0080	0.0060	0.0056	0.0126	0.0051	0.0076	0.0045	0.0062	0.0096	0.0109	0.0076
	tol=0.20	PSNR	38.33	37.44	37.40	36.79	36.30	37.63	38.92	36.83	37.48	36.20	36.13	38.38	36.18	37.23
		SSIM	0.9920	0.9895	0.9853	0.9895	0.9886	0.9869	0.9894	0.9920	0.9913	0.9878	0.9925	0.9899	0.9882	0.9895
		LPIPS	0.0197	0.0152	0.0172	0.0206	0.0181	0.0152	0.0285	0.0136	0.0208	0.0138	0.0155	0.0234	0.0278	0.0192
PixelGS+comp	tol=0.03	PSNR	51.51	52.17	52.54	52.46	52.37	51.86	52.26	51.82	52.23	52.10	52.67	50.48	51.90	52.03
		SSIM	0.9990	0.9980	0.9981	0.9991	0.9987	0.9977	0.9991	0.9986	0.9993	0.9977	0.9987	0.9988	0.9979	0.9985
		LPIPS	0.0020	0.0018	0.0015	0.0011	0.0011	0.0021	0.0020	0.0011	0.0012	0.0015	0.0010	0.0023	0.0021	0.0016
	tol=0.05	PSNR	47.56	48.03	48.67	48.18	48.10	47.94	48.39	47.82	48.18	47.85	48.14	46.88	47.60	47.95
		SSIM	0.9983	0.9970	0.9970	0.9984	0.9980	0.9964	0.9982	0.9980	0.9987	0.9963	0.9982	0.9979	0.9971	0.9977
		LPIPS	0.0048	0.0039	0.0033	0.0030	0.0027	0.0047	0.0055	0.0023	0.0033	0.0031	0.0025	0.0051	0.0050	0.0038
	tol=0.10	PSNR	42.41	42.18	42.73	41.97	41.85	42.11	42.78	41.65	42.24	41.20	41.50	42.00	41.61	42.02
		SSIM	0.9954	0.9932	0.9914	0.9950	0.9948	0.9913	0.9943	0.9952	0.9958	0.9915	0.9958	0.9945	0.9940	0.9940
		LPIPS	0.0123	0.0115	0.0101	0.0104	0.0086	0.0152	0.0164	0.0078	0.0106	0.0114	0.0084	0.0140	0.0164	0.0118
	tol=0.20	PSNR	37.54	36.39	36.83	36.25	35.38	36.64	37.40	35.45	36.41	35.67	34.96	36.72	36.75	36.34
		SSIM	0.9834	0.9817	0.9788	0.9833	0.9833	0.9781	0.9804	0.9860	0.9853	0.9815	0.9875	0.9804	0.9854	0.9827
		LPIPS	0.0298	0.0311	0.0292	0.0261	0.0263	0.0407	0.0376	0.0228	0.0284	0.0318	0.0232	0.0365	0.0394	0.0310

large-scale deployment where rapid compression of existing assets is paramount.

Table 3. Quantitative comparison across 13 scenes. We report PSNR \uparrow , SSIM \uparrow , and LPIPS \downarrow . “Base” refers to the original method, while “Comp.” denotes the application of our compression framework. For instance, “PixelGS Base” represents the vanilla PixelGS method, and “No SQ” indicates the removal of Scalar Quantization from EAGLES.

Method	Type	Metric	Bicycle	Bonsai	Counter	Drjohnson	Flowers	Garden	Kitchen	Playroom	Room	Stump	Train	Treehill	Truck	Mean
3DGS	Base.	PSNR	26.11	32.06	28.90	29.41	22.86	28.15	31.04	30.17	31.33	26.65	22.14	23.48	25.27	27.51
		SSIM	0.8103	0.9403	0.9007	0.9052	0.6929	0.8812	0.9161	0.9111	0.9133	0.7895	0.8110	0.7026	0.8723	0.8497
		LPIPS	0.1485	0.1240	0.1518	0.1728	0.2533	0.0949	0.1063	0.1540	0.1450	0.1813	0.1775	0.2389	0.1256	0.1595
	Comp.	PSNR	26.04	31.69	28.73	29.27	22.82	28.01	30.74	30.01	31.09	26.60	22.11	23.45	25.21	27.37
		SSIM	0.8092	0.9378	0.8975	0.9044	0.6917	0.8788	0.9139	0.9107	0.9108	0.7879	0.8099	0.7017	0.8707	0.8481
		LPIPS	0.1525	0.1282	0.1559	0.1761	0.2566	0.1004	0.1111	0.1558	0.1487	0.1878	0.1806	0.2416	0.1286	0.1634
MCMC	Base.	PSNR	27.21	32.65	29.34	29.35	23.28	29.76	32.06	29.94	32.13	27.84	22.71	24.29	26.43	28.23
		SSIM	0.8654	0.9476	0.9162	0.9024	0.7335	0.9269	0.9333	0.9112	0.9277	0.8443	0.8415	0.7379	0.9007	0.8761
		LPIPS	0.1054	0.1905	0.1854	0.2344	0.1835	0.0524	0.1208	0.2377	0.1988	0.1297	0.1816	0.1850	0.1084	0.1626
	Comp.	PSNR	27.11	32.21	29.17	29.14	23.25	29.55	31.64	29.67	31.82	27.77	22.64	24.25	26.33	28.04
		SSIM	0.8643	0.9443	0.9133	0.9013	0.7324	0.9250	0.9316	0.9107	0.9246	0.8429	0.8403	0.7369	0.8993	0.8744
		LPIPS	0.1110	0.1945	0.1890	0.2379	0.1880	0.0585	0.1246	0.2392	0.2009	0.1373	0.1852	0.1898	0.1117	0.1677
PixelGS	Base.	PSNR	26.74	32.34	29.17	28.10	22.91	29.32	31.54	29.91	31.23	27.19	22.26	23.35	25.47	27.66
		SSIM	0.8483	0.9453	0.9139	0.8876	0.7234	0.9215	0.9302	0.9044	0.9179	0.8197	0.8289	0.7095	0.8866	0.8644
		LPIPS	0.1131	0.1916	0.1825	0.2548	0.1787	0.0557	0.1194	0.2403	0.2104	0.1424	0.1783	0.1986	0.1208	0.1682
	Comp.	PSNR	26.63	31.82	28.97	27.99	22.89	29.09	31.14	29.74	30.89	27.12	22.22	23.32	25.38	27.48
		SSIM	0.8459	0.9415	0.9086	0.8867	0.7219	0.9182	0.9275	0.9040	0.9134	0.8173	0.8272	0.7074	0.8843	0.8619
		LPIPS	0.1198	0.1970	0.1874	0.2591	0.1835	0.0632	0.1245	0.2430	0.2153	0.1508	0.1824	0.2054	0.1252	0.1736
EAGLES	Base.	PSNR	26.31	31.24	28.32	29.32	22.74	28.53	30.50	30.22	31.43	26.97	21.43	23.80	25.01	27.37
		SSIM	0.8200	0.9368	0.8998	0.9083	0.6856	0.9001	0.9224	0.9128	0.9191	0.8032	0.7988	0.7134	0.8755	0.8689
		LPIPS	0.1754	0.2152	0.2148	0.2413	0.2793	0.0889	0.1373	0.2513	0.2235	0.1825	0.2369	0.2729	0.1647	0.2065
	No SQ	PSNR	26.54	32.00	28.94	29.03	23.01	28.88	31.11	29.96	31.35	27.09	21.62	23.77	25.29	27.58
		SSIM	0.8303	0.9410	0.9083	0.9031	0.7013	0.9086	0.9281	0.9085	0.9199	0.8102	0.8018	0.7127	0.8779	0.8578
		LPIPS	0.1562	0.2096	0.2024	0.2503	0.2618	0.0742	0.1289	0.2519	0.2205	0.1646	0.2325	0.2663	0.1624	0.1986